A comparison of fatigue crack growth performance of two aerospace grade aluminium alloys reinforced with bonded crack retarders

Syed, A, Zhang, X & Fitzpatrick, M

Original citation & hyperlink:
Syed, A, Zhang, X & Fitzpatrick, M 2017, 'A comparison of fatigue crack growth performance of two aerospace grade aluminium alloys reinforced with bonded crack retarders' *Fatigue and Fracture of Engineering Materials and Structures*, vol 41, no. 5, pp. (in press).
https://dx.doi.org /10.1111/ffe.12744
DOI 10.1111/ffe.12744
ISSN 8756-758X
ESSN 1460-2695
Publisher: Wiley

A comparison of fatigue crack growth performance of two aerospace grade aluminium alloys reinforced with bonded crack retarders

Abdul Khadar Syed, Xiang Zhang*, Michael E. Fitzpatrick

Faculty of Engineering, Environment and Computing, Coventry University, Coventry, CV1 5FB, UK

Email address: abdul.syed@coventry.ac.uk; xiang.zhang@coventry.ac.uk; michael.fitzpatrick@coventry.ac.uk

Abstract

To improve the fail-safety performance of integral metallic structures, the bonded crack retarder concept has been developed in recent years. This paper presents an experimental investigation on the effectiveness of bonded crack retarder on fatigue crack growth life in two aerospace aluminium alloys: 2624-T351 and 7085-T7651. M(T) specimens bonded with a pair of straps made of GLARE fibre-metal laminate were tested under the constant amplitude load. Although the bonded crack retarders increased the crack growth life in both alloys, the magnitude of life improvement is very different between them. Compared to unreinforced specimens, application of crack retarders has resulted in 90% increase in fatigue life in AA7085, but only 27% increase in AA2624. The significant difference in fatigue life improvement is owing to the material's intrinsic fatigue crack growth rate property, i.e. the Paris law constants C and n. Value of n for AA7085 is 1.8 times higher than that for AA2624. Therefore, AA7085 is much more sensitive to reductions in the effective stress intensity factor brought by the crack retarders; hence better life improvement.

Keywords

Aluminium alloys, Bonded crack retarders, Fatigue crack growth rate, Paris law, Stress intensity factor.

Nomenclature

a = Half crack length

A_{strap}, A_{Al} = Cross section area of strap and aluminium, respectively

E = Elastic or Young's Modulus

E_{strap}, E_{Al} = Elastic modulus of strap and aluminium, respectively

da/dN = Fatigue crack growth rate

K_{IC} = Plane-strain fracture toughness

β = Geometry factor

μ = Global stiffness ratio

ν = Poisson's ratio

σ_{ys} = Material yield strength under tension

σ_{max}, σ_{min} = Maximum and minimum applied stress

ΔK = Stress intensity factor range

σ_{UTS} = Ultimate tensile strength

M(T) = Middle crack Tension

1 Introduction

The key drivers for design and manufacturing of airframe structures are structural integrity, damage tolerance, and reduction of structure weight and manufacturing cost. In order to achieve these requirements, aircraft designers have been developing novel design features in conjunction with the development of innovative manufacturing processes and new generation of advanced alloys. One way to reduce the airframe weight and manufacturing cost is to adopt the concept of an integral metallic structure by using advanced manufacturing technologies such as welding, large-scale casting or extrusion, and/or high-speed machining. Additive manufacturing is the latest technology innovation enabling production of integral structures. Integral structures also have the benefits of reduction in part counts and simplification in inspections. However, a major concern is that they generally lack fail safety in the event of fatigue cracking compared to traditional build-up structures assembled by mechanical fasteners.

For passenger aircraft, airworthiness requirements for fail safety and damage tolerance are mandatory. Therefore, it is important to include fail-safe design features in integral metallic structures. A solution for this is to build local pad-ups, called crenulations, between the integral stiffeners [1]. These features decrease the fatigue crack growth rate under constant amplitude loading. A doubling of the fatigue life is obtained. Another solution is to incorporate adhesively bonded straps at selected locations acting as crack retarders, thus enhancing the fatigue performance [2-7]. Both solutions build crack retarders at the manufacturing stage before any fatigue crack is developed. They are different from other crack arresting techniques, such as stop hole at crack tips and bonded repair patches. This technical note is about the application of bonded straps to increase the local stiffness and bridge the wake of an advancing crack, thereby reducing the crack growth driving force and consequently the crack growth rates. However, thermal residual stresses and secondary bending resulting

from single sided strap bonding are a concern in bonded crack retarders [8-10]. Thermal residual stresses can be reduced by lowering the curing temperature; however, this will increase the curing time [11]. In application, curing at elevated temperature is a requirement based on aircraft operation conditions. Amongst various materials, the fibre-metal laminate GLARE has been shown to be most effective owing to its low density [12], low residual stress arising from curing straps at elevated temperature, and improved fatigue and impact performance [5, 12-16]. In previous work [3-6], application of GLARE bonded crack retarders showed large benefit in AA2024 and AA7085.

Advanced aluminium alloys have been developed with attractive properties of high strength, and/or better durability and damage tolerance. Currently there are three major groups of aluminium alloys that are used in airframes: Al-Cu (2xxx series alloys), Al-Zn (7xxx series alloys) and Al-Mg-Zn (6xxx series alloys). Among these, the Al-Cu and Al-Zn are of particular interest for aerospace load-bearing structures owing to their superior strength-to-weight ratio, machinability, fatigue and fracture toughness properties [17, 18]. AA7085-T7651 offers high strength and 2624-T351 has high damage-tolerance, making them primary candidate materials for airframes of next-generation aircraft [17, 18]. This paper discusses the effectiveness of bonded crack retarders on these two alloys. The significance of this paper also goes beyond bonded crack retarder design. As we strive to improve fatigue life by other technologies, e.g. laser shock peening, cold working, to introduce beneficial compressive residual stresses and to reduce the crack tip stress intensity factors, the degree of life improvement depends also on the material's intrinsic fatigue crack growth rate property, specifically the exponent of the Paris law.

2 Experimental procedure

Middle-crack tension (M(T)) specimens were machined from AA7085-T7651 and AA2624-T351. The thickness of all specimen substrates was 5 mm. GLARE 6/5 was chosen as the strap material, which consists of alternate layers of six aluminium alloy 2024-T3 sheets of 0.4-mm-thick each and five layers of FM94-S2 glass pre-preg (0.26-mm-thick each) consisting of unidirectional S2 glass fibres reinforced by FM94 epoxy. The geometry of the M(T) specimens bonded with a pair of GLARE straps is shown in Fig. 1. The geometry and dimension are the same for specimens made of two different substrate materials, AA8075 and AA2624.

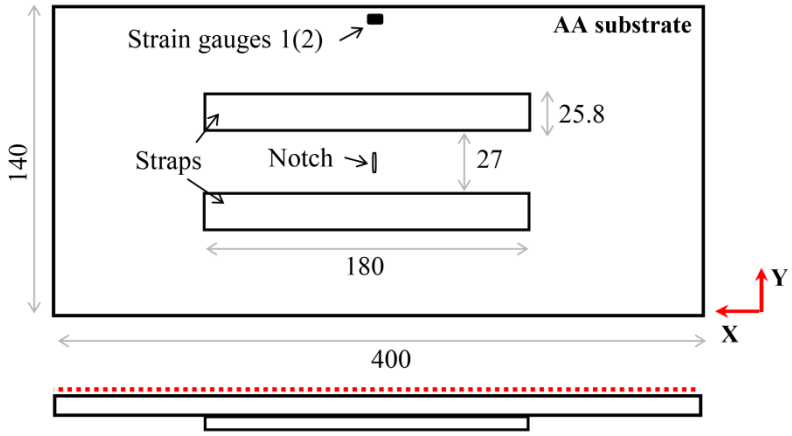

Fig 1: Geometry and dimensions of M(T) specimen reinforced with a pair of GLARE straps (unit: mm).

The mechanical properties of the GLARE laminate are E = 62 GPa, ν = 0.3. For 7085-T7651, the tensile yield strength σ_{ys} = 496 MPa (L-oriented), ultimate tensile strength σ_{UTS} = 517 MPa, elongation at failure = 9%, and L–T plane-strain fracture toughness K_{IC} = 32 MPa√m [17]. For 2624-T351, σ_{ys} =331 MPa, σ_{UTS}= 434 MPa, K_{IC} = 53 MPa√m [18]. Both materials have elastic modulus of 71 GPa. Prior to strap bonding, a starting notch of 16 mm length was introduced in the substrate using electro-discharge machining process.

Strap configuration was designed with a global stiffness ratio (μ) of 0.2, which is defined as [2]:

$$\mu = \frac{\sum(E_{strap}A_{strap})}{(E_{Al}A_{Al}) + \sum(E_{strap}A_{strap})} \qquad (1)$$

Prior to strap bonding, the substrates and the external aluminium sheets of GLARE were surface treated with Phosphoric Acid Anodizing (PAA) and with BR 127 modified epoxy phenolic primer to improve surface adhesion and corrosion-inhibiting properties. FM94® adhesive with a curing temperature of 120°C was used to bond the straps onto the substrate. The curing procedure is described in detail in [15]. After curing, the specimens were inspected using an ultrasonic phased array (C-scan) to ensure a defect-free bond.

Four specimens were tested for each substrate material: two with straps and two without. Specimens were subjected to constant amplitude loading at room temperature and the tests were performed according to the ASTM E-647 15e1 standard [19]. The maximum applied stress was 60 MPa with a stress ratio of 0.1. The loading frequency

was 10 Hz. Crack lengths were measured on the unreinforced side of the specimen with a travelling microscope. The anticipated crack path was polished to improve viewing of the crack.

3 Finite Element Analysis

Finite element analysis was performed using the commercial software ABAQUS. Material's elastic properties in [16] were used. The substrate, adhesive layer, and straps were modelled by 8-noded brick elements with reduced integration (C3D8R in ABAQUS). Following a mesh convergence study, element size of $1 \times 1 \times 1$ mm^3 was used. The substrate-adhesive and adhesive-strap interfaces were modelled by surface-based constraints, i.e. the nodes on the slave surface are set to deform with the closest node on the master surface using the ABAQUS TIE option. Measured residual stress filed owing to curing at 120°C is inputted in the model prior to the applied stress. According to [7], residual stresses (~20MPa) were inputted into the model via a predefined field. The specimen was then subjected to a far-field tensile stress of 60 MPa or 6 MPa (representing the maximum or minimum stresses in the fatigue crack growth test) at ambient temperature.

4 Results and discussion

Out-of-plane deformation occurred for this configuration. Firstly, elevated temperature cure of bonded straps resulted in substrate deformation owing to the mismatch of the coefficient of thermal expansion and elastic modulus between the strap and substrate materials. Deformation was measured by a co-ordinate measurement machine on the unreinforced side, along the longitudinal direction (X) of the specimen, as indicated with dotted lines on Fig. 1.

Schematic and measured deformation profiles are shown in Fig. 2. Both 7085 and 2624 substrates had exactly the same maximum deformation of 0.81 mm, approximately 16% of the substrate thickness. Secondly, the asymmetric (one-sided) strap configuration caused a shift of the specimen's neutral axis resulting in secondary bending when an in-plane stress is applied. To evaluate the magnitude of the secondary bending at the minimum and maximum applied stresses in the fatigue test, FE analysis was performed. At the minimum applied stress of 6 MPa, the specimen remains the same as its initial deformation shape (Fig. 2a), with a slightly smaller magnitude of deformation of 0.72 mm comparing to the initial deformation of 0.81 mm.

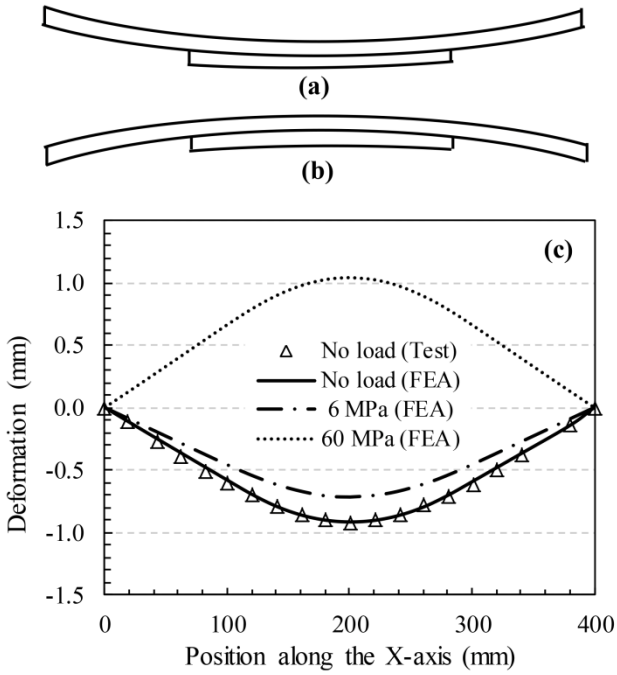

Fig 2: Out-of-plane deformation: (a) schematic of the specimen shape after curing and also at the minimum applied stress of 6 MPa; (b) at the maximum applied stress 60 MPa; (c) calculated and test measured deformation profiles.

At the maximum applied stress of 60 MPa, the specimen deformed in the opposite direction (Fig. 2b) with maximum magnitude of 1 mm. This significant change in the bending resulted in strain variation through the substrate thickness. A pair of strain gauges were used to measure the strain data on both sides of the specimens. The measured pure bending strain is 230 microstrain at the maximum applied stress. Using the Young's modulus of 71 GPa, the corresponding bending stress is 16 MPa acting on the unreinforced side of the substrate, which is 26% of the maximum applied stress during the fatigue testing. Since the fatigue loads are tension-tension, secondary bending does not cause instability. It should be noted that specimens made of 7085 and 2624 alloys were subjected to exactly the same magnitude of secondary bending.

Fig. 3 summarises the crack growth results for both alloys in the form of crack length vs. number of cycles, and crack growth rate vs. crack length. Averaged test data of two tests are shown in the Fig. 3. The application of the crack retarder has resulted in an increase in fatigue life for both alloys: with 27% and 90% life improvement for 2624 and 7085 respectively compared to unreinforced specimens. From Fig. 3b it is noticeable that the application of bonded crack retarders has resulted in a reduction in crack growth rate for both alloys. It can be seen that the beneficial effect of the strap is largely nullified when the crack tip is before the strap.

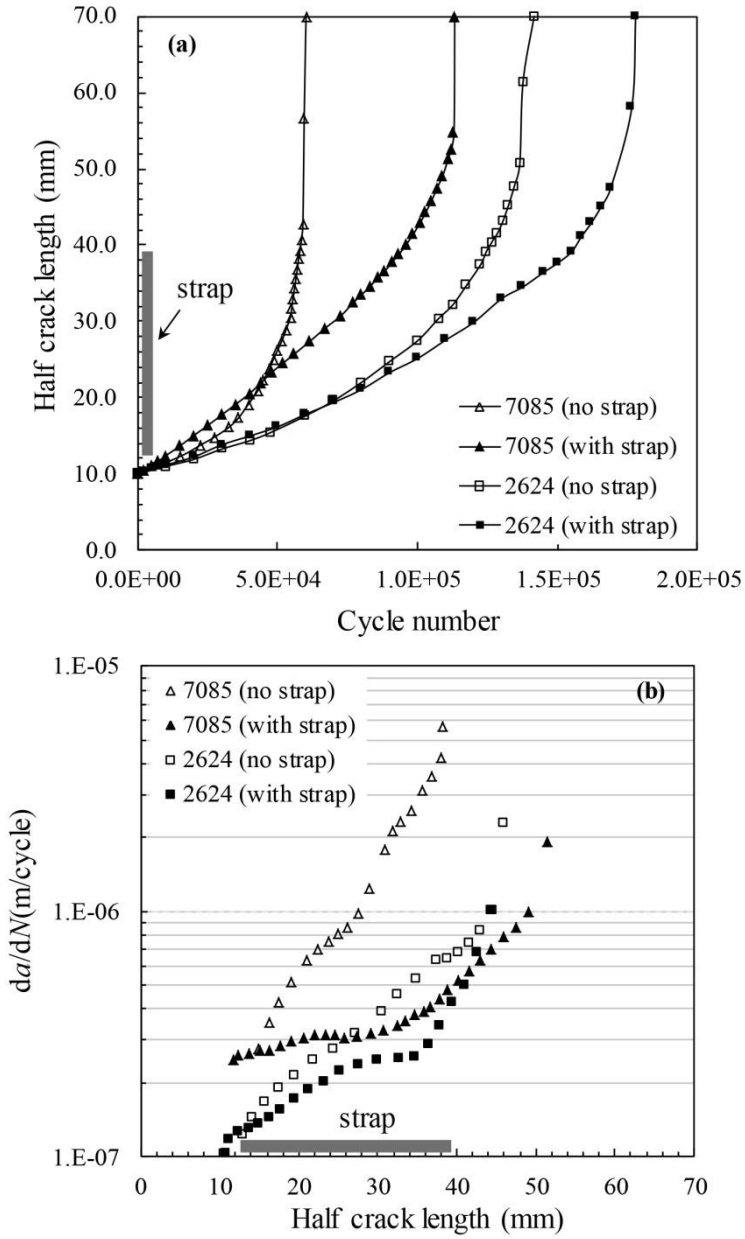

Fig 3: AA2624 vs. AA7085: (a) Half crack length vs. cycle numbers measured by fatigue tests, (b) crack growth rate vs. half crack length

This is owing to the effects of tensile residual stress and additional stress on the unreinforced side caused by the secondary bending. When the crack tip reaches the strap, a difference in fatigue crack growth rates can be observed compared to the unreinforced case. When the crack is under the strap, the effects of increased local stiffness and the strap bridging the wake of the crack cause reduction in the crack growth driving force, thereby reducing the crack growth rate. When the crack tip is beyond the strap, there is still significant benefit from the bonded crack retarder for the 7085 alloy but much less benefit for the 2624.

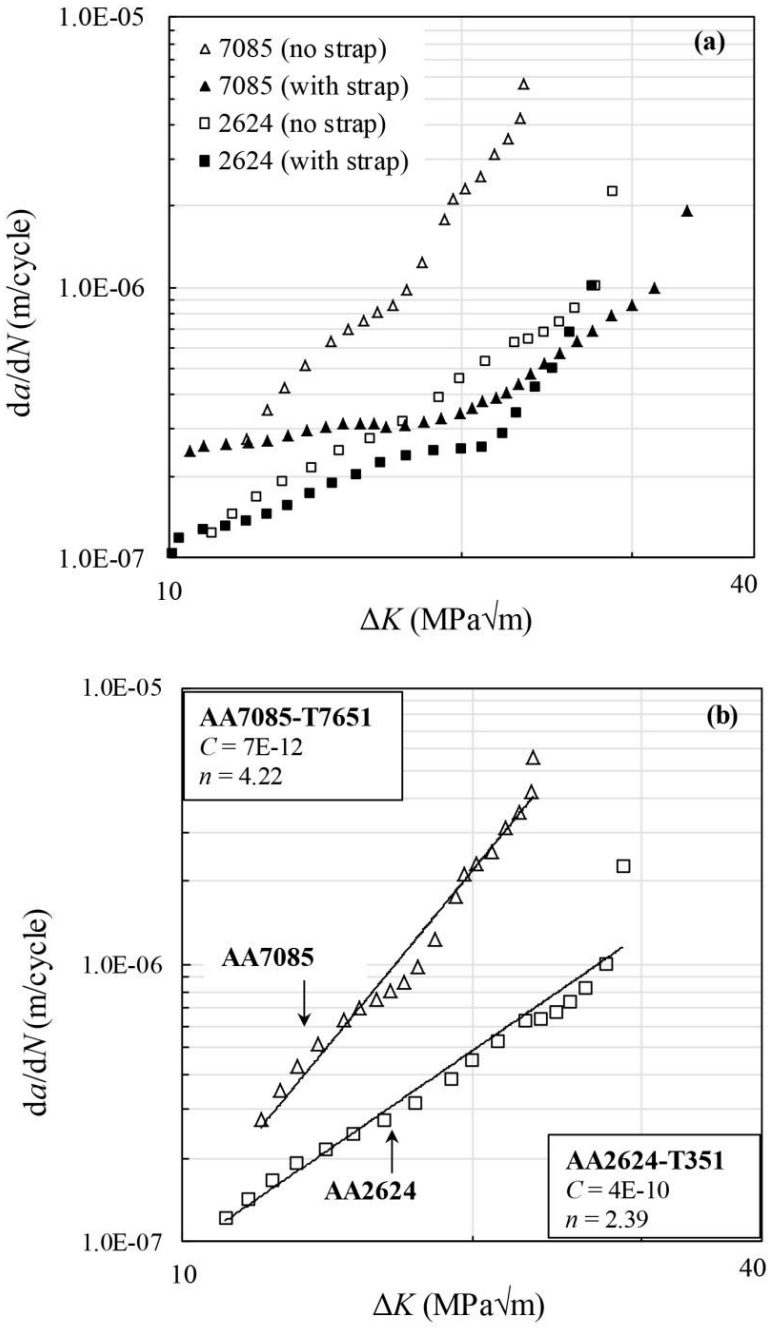

Fig 4: Fatigue crack growth rate vs. applied stress intensity factor range for: (a) specimens with and without straps (b) specimens without strap to determine the material's Paris law constants (values of these constants are inserted in the figure).

For the same geometry and same test conditions, the results show marked differences between the two alloys:

1) As expected, the 2624 alloy shows better fatigue performance than the 7085, by 200% in unreinforced specimens and 150% in strap reinforced specimens, reflecting the high damage tolerance property of the alloy.

2) The bonded crack retarder provides significantly greater life improvement for the 7085 alloy (90% improvement) compared to 2624 (27%).

The reason why the bonded crack retarder has not brought in the same level of life improvement in 2624 comparing to 7085 can be explained by looking at the materials' intrinsic fatigue crack growth rate properties. Fig. 4a shows crack growth rate vs. applied stress intensity factor range (d*a*/d*N* vs. Δ*K*) relationship for the two alloys, which are determined from the fatigue test results presented in Fig. 3a. This relationship is often described by the Paris law given by [20]:

$$da/dN = C\ (\Delta K)^n \qquad (2)$$

where, *C* and *n* are the material constants and stress intensity factor range Δ*K* is given by [21].

$$\Delta K = \beta\ (\sigma_{max} - \sigma_{min})\sqrt{\pi a} \qquad (3)$$

Measured values of *C* and *n* for the two materials are obtained by curve fitting the experiment data in Fig. 4a (for the unreinforced specimens) and are presented in Fig. 4b. It shows that both the *C* and *n* values differ significantly between the two alloys. Value of the exponent *n* is significantly lower in AA2624 than AA7085.

To predict the fatigue crack growth rate in reinforced specimens, an "effective" Δ*K* should be used in Paris law instead of the applied Δ*K*. Previous work on strap-reinforced AA2024 [2], AA7085 [6] and AA2624 [22] show that the effective Δ*K* is reduced significantly owing to the strap crack bridging mechanism, hence the consequent reduction of the crack growth rates in Fig. 4a under the same applied Δ*K*. In this study, AA2624 and AA7085 specimens have the same effective Δ*K* values because the effective Δ*K* term depends on the strap geometry and applied stress. Since fatigue crack growth rate is correlated by an exponential function of the effective Δ*K*, the value of the Paris law exponent *n* has a strong effect on the crack growth rate. Since the *n* value for AA2624 is only about 56% of that for AA7085, AA2624 is much less sensitive /reactive to the reduction in the effective Δ*K* term brought by bonded crack retarders. Since *C* is a coefficient in the Paris law, it has much less effect on fatigue crack growth rate comparing to exponent *n*.

5 Conclusions

This paper has highlighted the significant different gains in fatigue life improvement by applying the bonded crack retarder technology to two different aluminium alloys. For the same geometry and test conditions, the high-strength AA7085 alloy has

benefited considerably from the crack retarders, whereas the high-damage-tolerant AA2624 alloy only sees marginal benefit. It can be concluded that bonded crack retarders show higher benefit for materials with a lower Paris law exponent *n*.

Acknowledgment

The authors thank all the participants involved in this project including Alcoa and Canfield University. MEF is grateful for funding from the Lloyd's Register Foundation, a charitable foundation helping to protect life and property by supporting engineering-related education, public engagement and the application of research.

References

1. Ehrström, J.C., Van der Veen, S., Arsène, S., Muzzolini, R. (2005) Improving damage tolerance of integrally machined panels. Proceedings of 23rd ICAF symposium, 79−90.
2. Schijve, J. (1990) Crack stoppers and arall laminates. Engineering Fracture Mechanics., 37, 405–421.
3. Heinimann, M., Bucci, R., and Kulak, M., Garratt, M. (2005) Improving damage tolerance of aircraft structures through the use of selective reinforcement. Proceedings of 23rd ICAF symposium, 197−208.
4. Zhang, X., Boscolo, M., Figueroa-Gordon, D., Allegri, G., and Irving, PE. (2009) Fail-safe design of integral metallic aircraft structures reinforced by bonded crack retarders. Engineering Fracture Mechanics, 76, 114–133.
5. Irving, PE., Zhang, X., Doucet, J., Figueroa-Gordon, D., Boscolo, M., Heinimann, M., Shepherd, G., Fitzpatrick, ME., and Liljedahl, D. (2011) Life extension techniques for aircraft structures – Extending Durability and Promoting Damage Tolerance through Bonded Crack Retarders, Proceedings of 26th ICAF symposium, 753–770.
6. Boscolo, M., Allegri, G., and Zhang, X. (2008) Design and modelling of selective reinforcements for integral aircraft structures, AIAA journal, 46, 2323−2331.
7. Liljedahl, CDM., Fitzpatrick, ME., and Edwards, L. (2008) Residual stresses in structures reinforced with adhesively bonded straps designed to retard fatigue crack growth. Composite Structures, 86, 344–355.

8. Sabelkin, V., Mall, S., Hansen, M, Vandawaker, RM., Derriso, M. (2007) Investigation into cracked aluminum plate repaired with bonded composite patch. Composite Structures, 79, 55–66.
9. Hosseini-Toudeshky, H., Mohammadi, B. (2007). A simple method to calculate the crack growth life of adhesively repaired aluminum panels. Composite Structures, 79, 234–241.
10. Hosseini-Toudeshky, H., Sadeghi, G., Daghyani, HR. (2005). Experimental fatigue crack growth and crack-front shape analysis of asymmetric repaired aluminium panels with glass/epoxy composite patches. Composite Structures, 71, 401–406.
11. Ong, CL., Shen, SB. (1992). The reinforcing effect of composite patch repairs on metallic aircraft structures. International Journal of Adhesion & Adhesives, 12 (1), 19−26.
12. Vermeeren C.A.J.R. (2002). Around Glare – A New Aircraft Material in Context. Kluwer Academic Publishers, Dordrecht.
13. Syed, AK., Fitzpatrick, ME., Moffatt, JE. (2014) Evolution of residual stress during fatigue crack growth in an aluminium specimen with a bonded crack retarder. Composite Structures, 117, 12–16.
14. Syed, AK., Fitzpatrick, ME., and Moffatt, JE. (2014) Effect of thermal residual stresses on bonded structures containing cold expanded and bolted holes. Advanced Materials Research, 996, 682–687.
15. Syed, AK., Fitzpatrick, ME., Moffatt, JE., Doucet, J., and Durazo-Cardenas, I. (2015) Effect of impact damage on fatigue performance of structures reinforced with GLARE bonded crack retarders. International Journal of Fatigue, 80, 231−237.
16. Syed, AK., Zhang, X., Moffatt, JE., and Fitzpatrick, ME. (2017) Effect of temperature and thermal cycling on fatigue crack growth in aluminium reinforced with GLARE bonded crack retarders. International Journal of Fatigue, 98, 53−61.
17. https://www.alcoa.com/mill_products/catalog/pdf/AAP7085-factsheet.pdf, Accessed on 1st August 2016.
18. https://www.alcoa.com/mill_products/catalog/pdf/AAP2624-factsheet.pdf, Accessed on 1st August 2016.

19. ASTM E647-15e1, Standard test method for measurement of fatigue crack growth rates. ASTM International 2015.
20. Paris, PC., and Erdogan, F. (1963) A Critical Analysis of Crack Propagation Laws. Journal of Basic, Engineering, 85, 528−534.
21. Anderson, TL. Fracture Mechanics: Fundamentals and applications (2005), Taylor and Francis, UK.
22. Doucet, J., Zhang, X., Irving, PE. (2013) Fatigue modelling of aluminium plates reinforced with bonded fibre metal laminates. International Journal of Structural Integrity 4 (4), 416−428.